PHYSICAL REVIEW B VOLUME 58, NUMBER 21 1 DECEMBER 1998-I

Far-infrared study of the Jahn-Teller-distorted C_{60} monoanion in C_{60}-tetraphenylphosphoniumiodide

V. C. Long and J. L. Musfeldt
Department of Chemistry, State University of New York at Binghamton, Binghamton, New York 13902-6016

K. Kamarás
Research Institute for Solid State Physics, Hungarian Academy of Sciences, H 1525 Budapest, Hungary

A. Schilder and W. Schütz
Experimentalphysik II und BIMF an der Universität Bayreuth, 95440 Bayreuth, Germany

(Received 12 May 1998)

We report high-resolution far-infrared transmission measurements on C_{60}-tetraphenylphosphoniumiodide as a function of temperature. In the spectral region investigated (20–650 cm^{-1}), we assign intramolecular modes of the C_{60} monoanion and identify low-frequency combination modes. The well-known $F_{1u}(1)$ and $F_{1u}(2)$ modes are split into doublets at room temperature, indicating a D_{5d} or D_{3d} distorted ball. This result is consistent with a dynamic Jahn-Teller effect in the strong-coupling limit or with a static distortion stabilized by low-symmetry perturbations. The appearance of silent odd modes is in keeping with symmetry reduction of the ball, while activation of even modes is attributed to interband electron-phonon coupling and orientational disorder in the fulleride salt. Temperature dependences reveal a weak transition in the region 125–150 K in both C_{60}^- and counterion modes, indicating a bulk, rather than solely molecular, effect. Anomalous softening (with decreasing temperature) in several modes may correlate with the radial character of those vibrations. [S0163-1829(98)03245-7]

I. INTRODUCTION

The discovery of a new allotropic form of carbon, C_{60},[1] and its subsequent production in macroscopic quantities,[2] have led to investigations of numerous fullerene-related materials.[3] Among these, the fulleride salts of alkali metals and alkaline earths exhibit superconductivity and a variety of phase transitions.[3] Recently, fully ionic C_{60}-tetraphenylphosphonium- and arsonium-halides were electrocrystallized and found to be air stable.[4,5] These latter materials have excited interest as prototypical systems of the isolated C_{60} monoanion in a crystalline environment.[6–12]

The aforementioned charge-transfer salts, $(Ph_4X)_2YC_{60}$ (with X=P or As and Y=I, Br, or Cl), are isostructural members of the tetragonal[13] space group $I_{4/m}$.[4,5] Singly charged C_{60} and halide anions occupy vertices of interpenetrating tetragonally distorted tetrahedra. The C_{60}^- balls are well separated and surrounded in near cubic symmetry by the large Ph_4X^+ counterions.[4,5] Recent elemental analysis shows that the iodide-containing compound is actually a mixed salt with chloride ions randomly substituted at halide sites, due to Cl incorporation from solvents during crystal growth.[14] The $I_{4/m}$ space group sustains two geometrically equivalent orientations of the C_{60}^- ball at 90 degrees relative to each other, resulting in local orientational disorder that is probably dynamic in nature.[4,5] Room-temperature rotation of the anion balls is indicated by rotational narrowing of the NMR line,[10,15] although other authors dispute this claim.[9]

Experiment shows that electronic and vibrational structures of the C_{60} anion in the $(Ph_4X)_2YC_{60}$ salts are minimally perturbed by the counterion environment.[9,12] A complex electronic absorption between 900 and 1200 nm (absent in C_{60}) resembles that found in electrochemically generated C_{60}^- and exhibits little sensitivity to X or Y constituents.[9,12] Similarly, the fundamental infrared (IR) vibrations show little dependence on the nature of the counterion.[9,12] Until now, attention has focused on two of the four IR-active fundamental modes, $F_{1u}(3)$ and $F_{1u}(4)$, which resonate in the middle infrared.[8,9,12,16] Whereas in pristine C_{60} these modes occur at 1182 and 1428 cm^{-1}, in $(Ph_4P)_2YC_{60}$ they downshift to 1179 and 1394 cm^{-1} (1390 cm^{-1} in X=As), respectively. The slight redshift of $F_{1u}(3)$ is attributed to increased intermolecular distances,[8] whereas the pronounced red shift and enhanced oscillator strength of $F_{1u}(4)$ are ascribed to the charged-phonon mechanism.[8,9,12] This mechanism is well known in the alkali-doped fullerides, where extra charge on the C_{60} ball causes coupling of the F_{1u} phonons to the doping-induced electronic transitions, resulting in a downshift and enhancement of the $F_{1u}(2)$ and $F_{1u}(4)$ modes.[17,18]

The Jahn-Teller effect (JTE) is another expected manifestation of electron-phonon coupling in the charged C_{60} ball.[19] Symmetry analysis predicts that H_g vibrational modes couple to the highest occupied molecular orbital (t_{1u}) of C_{60}^-, causing ellipsoidal Jahn-Teller (JT) distortions of the ball. Calculated symmetry reductions to D_{5d}, D_{3d}, or D_{2h} point groups all yield small JT stabilization energies,[20–23] and dynamic conversions among the distortions may occur.[20] EPR and near-IR investigations of frozen C_{60}^- solutions are cited as evidence of different point-group distortions, sensitivity of the anion to its environment, and both dynamic and static Jahn-Teller effects.[24–29] A recent CW EPR study of crystalline $(Ph_4P)_2IC_{60}$ reports a transition from a dynamic to

static JTE near 140 K, manifest in g-factor splitting and bandwidth narrowing at low temperature.[6,11,30] Pulsed EPR measurements on the chloride-containing salt show Orbach-type spin-lattice relaxations, consistent with JT vibronic excitations.[31]

$(Ph_4P)_2IC_{60}$ can be compared to other solid-state fullerene materials with regards to the charge and symmetry states of the ball and the degree of separation between balls. The A_nC_{60} alkali-metal doped fullerides contain the negatively charged C_{60} ball (charge$=n$) which is subject to a JTE for $1 \leqslant n \leqslant 5$.[22] With the exception of recent NMR results on Rb_4C_{60}, indicating JT splitting of the t_{1u} level,[32] there are no reports of Jahn-Teller distortions of the anion in these materials. Center-to-center distances of the balls are relatively smaller in the alkali fullerides, e.g., ≈ 10 Å in A_3C_{60} (Ref. 33) compared to 12.5 Å in $(Ph_4P)_2IC_{60}$.[4] This reduced separation allows for weak cooperative effects among the balls in the A_nC_{60} materials, whereas the large organic cations in $(Ph_4P)_2IC_{60}$ effectively isolate the balls from each other. In the polymer and dimer phases of the A_1C_{60} compounds, the balls are bonded to one or more of their neighbors, thus reducing the molecular symmetry to D_{2h} and even lower.[34–36] Similar structurally induced symmetry reductions are found in the high-pressure/high-temperature polymerized fullerites, in which the balls remain neutral.[34,37] The high-temperature (>400 K) fcc A_1C_{60} phase is the most similar to $(Ph_4P)_2IC_{60}$ in that both contain the singly charged ball in a very symmetric environment, although the balls separations are quite different.

Infrared vibrational spectroscopy is well suited to the study of molecular symmetry and symmetry reductions, and has been used extensively to investigate C_{60} and the alkali fullerides.[3,38] In this article, we report a high-resolution far-infrared (FIR) study of $(Ph_4P)_2IC_{60}$ as a function of temperature (T), with particular focus on the $F_{1u}(1)$ and $F_{1u}(2)$ fundamental modes, which have not been previously investigated. Thus, we supplement the vibrational studies reported to date[8,9,12,16] and complement the previous EPR temperature dependence work.[6,11,31]

II. EXPERIMENTAL METHOD

Small single crystals of $(Ph_4P)_2IC_{60}$, grown by electrocrystallization techniques,[4] were ground with paraffin[39] at 77 K. This mixture was compressed under vacuum at 1.5 kbar to form an isotropic pellet, approximately 0.2 mm thick and 2.5% by weight concentration. Commercially obtained Ph_4PI was similarly processed into two pellets (with concentrations optimized for different transmittance regimes) to provide reference spectra of the Ph_4P^+ counterion. A thin C_{60} film, deposited on a gold film and glass substrate, was measured in reflectance geometry, which yielded the equivalent of a double transmittance spectrum. Samples were evacuated for several hours in high vacuum before measurements.

We made infrared transmittance measurements on a Bruker 113V Fourier-transform infrared spectrometer, using the room-temperature or low-temperature apertured beam as a reference. A series of four different beamsplitters covered the spectral region 20–650 cm^{-1} and a B-doped Si bolometer detector, cooled to 4 K, provided extra sensitivity. Two detector filters (16 and 103 μm) were employed in appropriate regimes. The T dependence of $(Ph_4P)_2IC_{60}$ was measured with high resolution (0.3 cm^{-1}) in order to follow fine splitting or frequency shifts of the peaks. Other scans used 1 or 2 cm^{-1} resolution, as needed. An open-flow cryostat, equipped with standard cryogenic accessories, provided T control between 12 and 300 K.

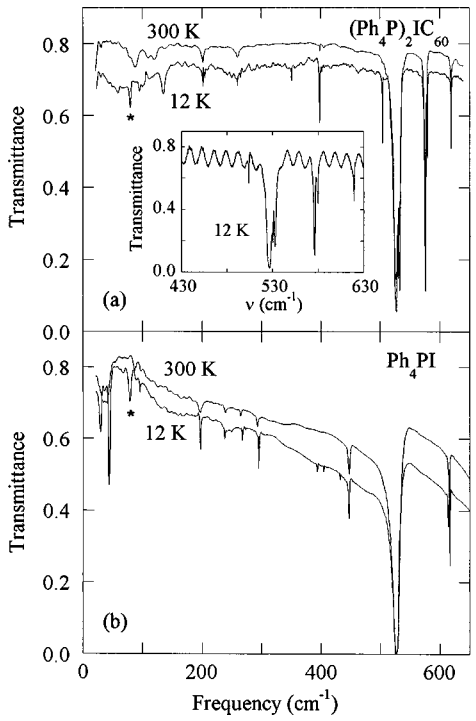

FIG. 1. Room-temperature and low-temperature transmittance versus frequency of (a) $(Ph_4P)_2IC_{60}$ and (b) Ph_4PI (* indicates a paraffin mode). Data have been treated to remove interference fringes as described in the text. The inset in (a) shows typical fringes present in the untreated data.

Strong interference fringing[40] [see inset to Fig. 1(a)] necessitated intensive data treatment to extract the weaker features of the spectrum. We fit successive regions of the data to a series of sine curves plus a linear background. After subtraction of the fits, we smoothed the result with a moving average algorithm, reinserted narrow peaks that had been oversmoothed, and finally resmoothed the overlap regions where peaks were reinserted. Low-temperature $(Ph_4P)_2IC_{60}$ data were renormalized in order to account for possible small misalignments of the cryostat. Detailed temperature dependences of the strong transmission peaks were plotted and analyzed using the untreated data (Figs. 2–5).

III. RESULTS

A. Peak assignments

Figure 1 shows the room temperature (RT) and low-temperature transmission spectra, between 20 and 650 cm^{-1}, of $(Ph_4P)_2IC_{60}$ (upper panel) and Ph_4PI (lower panel). The weaker modes of both the $(Ph_4P)_2IC_{60}$ and Ph_4PI spectra are strengthened at low T, while the overall slope and level stay nearly the same as in the RT spectra. Of the two F_{1u} modes that appear in this frequency regime, $F_{1u}(1)$ is overlapped

TABLE I. $(Ph_4P)_2IC_{60}$ and Ph_4PI low-temperature mode identification. *s* indicates strong, *m* indicates medium, and *w* indicates weak.

Ph_4PI mode (cm^{-1})	Strength	Average low-*T* behavior		$(Ph_4P)_2IC_{60}$ mode (cm^{-1})	Strength	Average low-*T* behavior
197.1	m	Hardens	↔	201.5, 205.2	w	Splits, hardens
237.6	w	Softens				
267.5	w	Hardens				
				260.3, 264.7	**w**	**Splits, hardens**
295.1	m	Hardens				
				350.7	**w**	**Softens**
393.6	w	Low T only				
				398.0, 398.5	**m**	**Splits, softens**
404.6	w	Low T only	↔	406.2	w	Hardens
432.4	w	Low T only				
447.0	m	Softens				
				503.9	**m**	**Softens**
				518.8, 520.2	**m**	**Low T only**
526.3, 529.3	s	Hardens	↔	526.7, 530.1	s	Hardens
				525,[a] **532.7**	s	**Hardens**
				576.1, 579.7	s	**Hardens**
613.8, 616.7	m	Hardens	↔	619.2	m	Hardens

[a]Expected position; the mode itself is obscured by the strong counterion feature at 526 cm^{-1}.

by the strong counterion mode at 527 cm^{-1}, while $F_{1u}(2)$ is observed at the usual 576 cm^{-1} location, in a region free of counterion vibrations.

The vibrational spectrum of molecular C_{60} contains no modes between 60 and 273 cm^{-1}, the highest intermolecular and lowest intramolecular vibrations, respectively.[3] Furthermore, due to the high symmetry of the fullerene ball, the IR spectrum of solid C_{60} contains no strong IR-active modes below 525 cm^{-1}, only weakly activated ones associated with crystal-field effects in the solid.[41–43] In comparison, the spectrum of the lower symmetry counterion [Fig. 1(b)] is quite complex, with several intramolecular modes of moderate strength throughout the 200–500 cm^{-1} region. The $(Ph_4P)_2IC_{60}$ spectrum [Fig. 1(a)] is likewise rich with structure in this regime, reflecting the counterion contributions as well as newly activated modes of the C_{60}^- anion, which must be carefully distinguished.

Table I lists all intramolecular modes in the low-*T* spectra of the counterion and $(Ph_4P)_2IC_{60}$, along with their approximate strength and average frequency shift at low temperature. The ↔ symbol indicates that the $(Ph_4P)_2IC_{60}$ mode shown on the right has its origin in the counterion mode shown on the left, based on similarities in frequency (shifted by less than 6 cm^{-1}), magnitude, and *T* dependence. $(Ph_4P)_2IC_{60}$ modes with no counterpart in the counterion (in bold) are assumed to be modes of the C_{60}^- ball. Several counterion modes are absent in the salt, probably diminished due to the different environment or shifted in frequency. Note that $(Ph_4P)_2IC_{60}$ contains chloride substituted on some of the iodide sites,[14] while Ph_4PI (used as a reference for the counterion) contains no chloride. We do not expect any significant difference in counterion modes of the different halide salts, however.[12]

Of the eleven intramolecular $(Ph_4P)_2IC_{60}$ vibrations (doublets are taken as one mode and referred to by the lower frequency peak), four are easily attributable to counterion vibrations which shift to slightly higher energy in the fulleride salt. Two modes of $(Ph_4P)_2IC_{60}$ have nearby counterparts in the counterion but are attributed to C_{60}^- due to logical assignments of C_{60} fundamentals, as discussed in Sec. IV A. One of these is a weak mode at 260 cm^{-1}, slightly lower in energy than the closest counterion feature at 267 cm^{-1}. This redshift relative to the counterion vibration distinguishes it from the prevailing pattern and reinforces our identification of it as an activated mode of the anion ball. The other is a moderately strong mode at 398 cm^{-1} whose intensity is much greater than the nearby counterion mode, further motivating the C_{60}^- assignment. Finally, we include the 504 cm^{-1} mode of $(Ph_4P)_2IC_{60}$ among those of the C_{60} anion, since it has no identifiable counterpart among the counterion modes, but this assignment is called into question under closer examination in Sec. IV A.

In the low-energy region of the low *T* Ph_4PI spectrum [Fig. 1(b)] there are two strong lattice modes at 29 and 44 cm^{-1}, which split and gain intensity from a broader RT mode. These modes do not reappear in the $(Ph_4P)_2IC_{60}$ spectrum, however, probably because the counterions are separated in the salt by large C_{60}^- balls.[4,44] Both low-*T* spectra contain a paraffin peak at 79 cm^{-1} and, at slightly higher energy, some features which we attribute to combination modes (correlated translations of the C_{60}^- ball and counterion, or Cl or I anion).

B. Temperature dependence

Expanded-scale plots of the high-resolution data display the fine features and temperature dependences of the various multiplet $(Ph_4P)_2IC_{60}$ modes. Figures 2, 3, and 4 show the intense doublet at 576 cm^{-1}, the strong overlapped absorption at 525 cm^{-1}, and the moderately strong doublet at

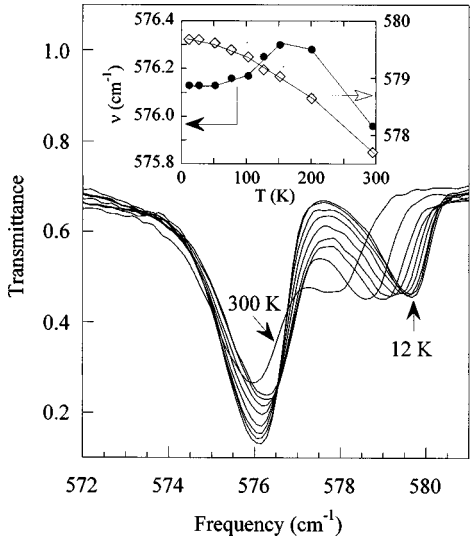

FIG. 2. Temperature dependence of the $F_{1u}(2)$-derived doublet. The inset displays frequency versus temperature of the two transmission minima (high and low ν sides of the doublet), with solid lines to guide the eye.

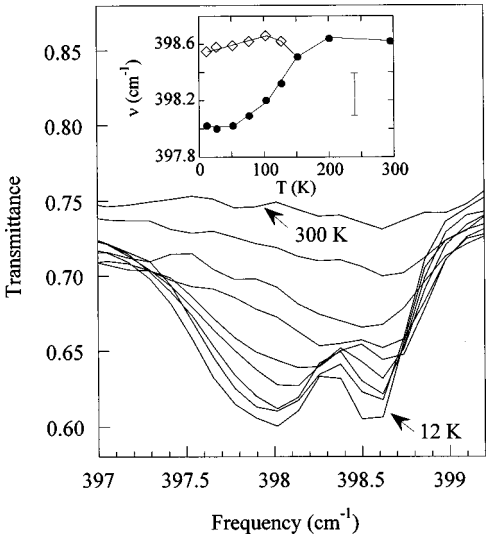

FIG. 4. Temperature dependence of the $G_u(1)$-derived mode. The inset plots frequency versus temperature for the transmission minima of the doublet, with solid lines to guide the eye. The error bar reflects the 0.3 cm^{-1} measurement resolution.

398 cm^{-1}, respectively. The insets plot frequencies (ν) of the transmission minima[45] versus temperature, with solid lines to guide the eye along the sometimes subtle trends. Whereas the measurement resolution was 0.3 cm^{-1}, the limited scatter in the ν vs T plots suggests a significantly smaller uncertainty.

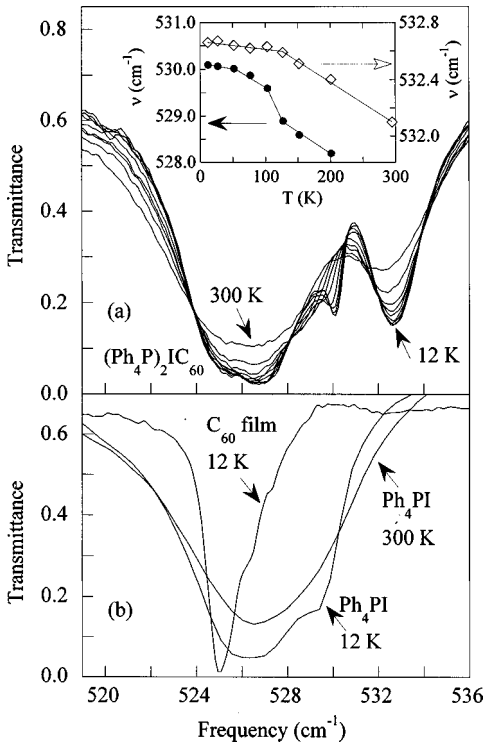

FIG. 3. Temperature dependences of (a) the $(Ph_4P)_2IC_{60}$ multiplet and (b) the pristine C_{60} and Ph_4PI absorbances which contribute to it. The inset in (a) shows frequency versus temperature for the high ν side of the $F_{1u}(1)$-derived doublet (open diamonds) and the 530 cm^{-1} counterion feature (solid circles), with solid lines to guide the eye.

Figure 2 displays the T-dependent frequency shifts of the 576 cm^{-1} $F_{1u}(2)$-derived mode, which is split into a doublet in $(Ph_4P)_2IC_{60}$. Both sides of the doublet exhibit anomalous T dependence in the 125–150 K region. With decreasing T, the low ν side of the doublet initially hardens, then softens when T falls below 150 K, with the maximum change in slope occurring near 125 K. In contrast, the high ν side hardens monotonically, although an inflection point appears near 150 K (obvious in a plot of the second derivative of ν with respect to T, not shown).

Figure 3 shows the 526 cm^{-1} multiplet structure of $(Ph_4P)_2IC_{60}$ (upper panel), which is a complicated overlapping of counterion, C_{60}, and activated anion modes, as deduced from the individual absorbances of pristine C_{60} and Ph_4PI (lower panel). The structure of the low-T counterion peak suggests an incipient splitting which, in the salt, produces the separate counterion mode at 530 cm^{-1}. A weak additional structure at 525 cm^{-1} in the $(Ph_4P)_2IC_{60}$ multiplet probably reflects the contribution of the $F_{1u}(1)$ mode, appearing unshifted from the usual low-T fullerene frequency. The feature at 533 cm^{-1} in $(Ph_4P)_2IC_{60}$ is clearly a mode activated in the salt. From the combined structure (the obscured 525 cm^{-1} mode and the 533 cm^{-1} peak) we infer doublet splitting of the $F_{1u}(1)$ mode. The inset shows the temperature behaviors of the 530 cm^{-1} counterion mode and the high ν side of the $F_{1u}(1)$ doublet at 533 cm^{-1}. Both of these exhibit anomalies in the 125–150 K region: the C_{60}^- mode changes slope (flattens below 125 K) and the counterion mode contains a strong inflection point near 150 K. Unfortunately, the T dependence of the low ν side of the $F_{1u}(1)$ doublet cannot be followed due to overlap of the strong (T-independent) counterion absorption at 527 cm^{-1}.

Figure 4 displays the temperature dependence of the 398 cm^{-1} mode, a vibration which we believe is newly activated in the charged C_{60}^- ball. To within the resolution of our measurements, the room-temperature singlet persists down to 150 K, at which point it splits into a doublet, with a maximum splitting of $\approx$0.5 cm^{-1}. The high ν side of the

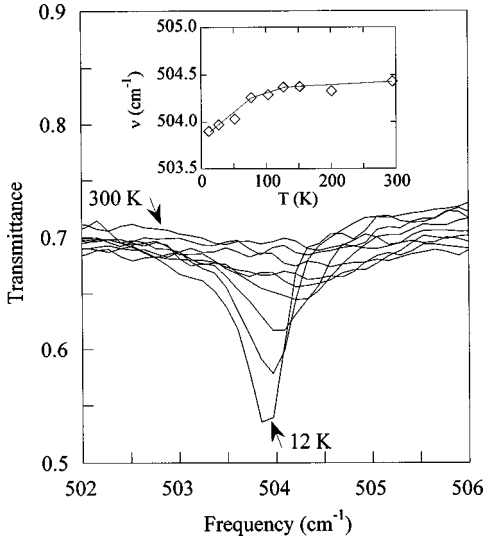

FIG. 5. Temperature dependence of the unidentified 504 cm^{-1} mode. The inset shows the frequency shift of the transmission minimum, with solid lines to guide the eye.

doublet is almost independent of T, while the dominant low ν side softens strongly just below the transition and then levels out.

The temperature dependence of the 504 cm^{-1} singlet mode, whose origin remains a mystery, is shown in Fig. 5. The frequency of this mode remains very flat down to 125 K, then softens with decreasing T. This feature also exhibits noticeable narrowing at low T and a sharp increase in intensity below 125 K.

Detailed temperature behaviors of other $(Ph_4P)_2IC_{60}$ modes (both C_{60}^- and counterion features) also point to some sort of weak transition between 125 and 150 K, as enumerated below. The weak C_{60}^- mode at 351 cm^{-1} first softens, then hardens, and finally levels out near 125 K. Another weak anion mode, at 260 cm^{-1}, splits into a doublet at low T (between 100 and 200 K). The counterion mode at 201 cm^{-1} splits into a doublet below 125 K and the minute frequency shift of the 619 cm^{-1} counterion mode flattens out near 125 K.

As expected, the C_{60}^- modes increase in intensity and decrease in linewidth with decreasing temperature. The intensity effect is weak-to-moderate in the F_{1u}-derived (and counterion) modes and strong in some of the newly activated C_{60}^- modes, which are barely observable at room temperature. Plots of the integrated peak intensities versus T (not shown) display no anomalies, except for the unidentified 504 cm^{-1} mode, as previously mentioned. Linewidth narrowing is also most dramatic in that mode and relatively modest in other modes.

C. Low-energy modes

Analysis and assignment of the low-energy modes of $(Ph_4P)_2IC_{60}$ were complicated by the fact that in most cases the peak magnitudes were less than the amplitude of the interference fringes, while the peak widths were often on the order of the fringe period. Nevertheless, independent treatment of two separate data sets taken at different resolutions (1 and 2 cm^{-1}) resulted in good qualitative agreement in

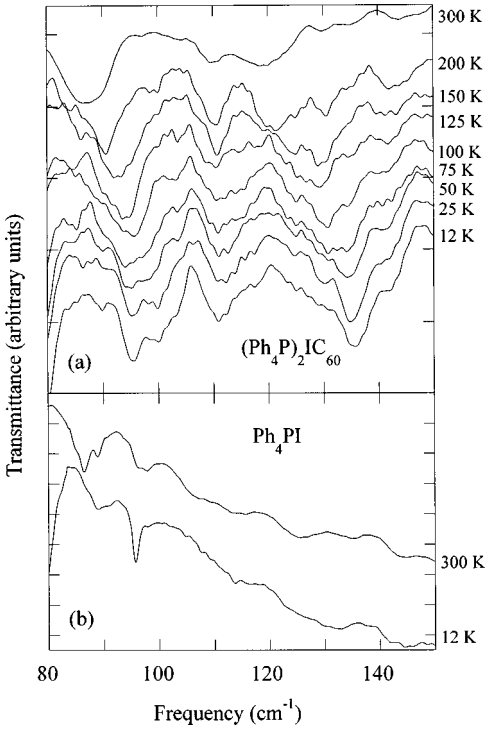

FIG. 6. Temperature dependence of the low energy combination modes of (a) $(Ph_4P)_2IC_{60}$ and (b) Ph_4PI; the curves are offset for clarity.

appearance and T dependence of the $(Ph_4P)_2IC_{60}$ low-energy modes. Hence, we are confident in the approximate frequencies and temperature behavior of these modes, with the exception of some ambiguity in the location of the mode between 110 and 120 cm^{-1}.

Figure 6 displays the temperature dependence of the low-energy spectra of $(Ph_4P)_2IC_{60}$ (upper panel) and Ph_4PI (lower panel), taken at 1 cm^{-1} resolution. At least two of the three $(Ph_4P)_2IC_{60}$ modes between 90 and 135 cm^{-1} are unique to the salt, probably combination modes involving both large ions, and possibly the halide ions, in the vibration. One of these may derive from the low-T Ph_4PI vibration at 95 cm^{-1}. Since different packing of counterions in the fulleride salt may shift or diminish such a feature, we cannot conclusively assign the $(Ph_4P)_2IC_{60}$ and Ph_4PI 95 cm^{-1} modes to the same origin.

IV. DISCUSSION

A. Symmetry assignments

Table II lists the C_{60}^- modes of $(Ph_4P)_2IC_{60}$ which appear in the FIR spectrum, along with the nearby fundamental and overtone modes of the neutral fullerene.[41,42] As mentioned previously, the F_{1u} modes appear at the usual frequencies, whereas the other five modes are activated from even and odd silent vibrations of C_{60}. Unless the ball symmetry loses its inversion center, the rule of mutual exclusion of IR- and Raman-active modes is expected to hold. Assignments of the 351 and 398 cm^{-1} features to $F_{2u}(1)$ and $G_u(1)$, respectively, obey the parity selection exclusion rule, and therefore seem quite reasonable. Moreover, these C_{60}^- modes appear very close in frequency (slightly redshifted) to the C_{60}

TABLE II. Correspondence of low-T $(Ph_4P)_2IC_{60}$ modes and C_{60} fundamental modes. C_{60} mode assignments consistent with both Martin *et al.* (Ref. 42) and Wang *et al.* (Ref. 41) unless otherwise noted.

$(Ph_4P)_2IC_{60}$ mode (cm^{-1})	Strength	C_{60} fundamental mode (cm^{-1})	C_{60} mode assignment
260 doublet	w	273	$H_g(1)$
351 singlet	w	353	$F_{2u}(1)$
398 doublet	m	403	$G_u(1)$
504 singlet	m	497, 502[a]	$A_g(1)$, $F_{1g}(1)$[a]
519 doublet	w	533[b]	$H_g(1)\otimes H_g(1)$[b]
525 doublet	s	526	$F_{1u}(1)$
576 doublet	s	576	$F_{1u}(2)$

[a]Assignment from Wang *et al.* (Ref. 41), in disagreement with Martin *et al.* (Ref. 42).
[b]Assignment from Martin *et al.* (Ref. 42), absent from the assignments of Wang *et al.* (Ref. 41).

modes. The symmetry assignment of the 398 cm^{-1} doublet in $(Ph_4P)_2IC_{60}$ is supported by observation of a 390 cm^{-1} triplet (consistent with expected D_{2h} symmetry) in polymeric RbC_{60},[35] which presumably originates from the same $G_u(1)$ mode. We note that some odd silent vibrations found in this region of the C_{60} spectrum are not observed: $H_u(1)$ at 343 cm^{-1} (Refs. 41, 42) and $H_u(2)$ at 580 cm^{-1} (Ref. 42) (the latter may be hidden under the high ν side of the 576 cm^{-1} doublet, causing asymmetry in that mode shape). On the other hand, a weak low-T doublet at 665 cm^{-1}, although strictly speaking out of the reliability range of our beamsplitter, suggests an activation of $H_u(3)$ [found in C_{60} at 668 cm^{-1} (Ref. 42)].

Weak breaking of parity selection may occur in some cases due to electron-phonon coupling, as discussed later in more detail.[46,47] We attribute the weak modes at 260 and 519 cm^{-1} to activation of the $H_g(1)$ mode and its overtone, $H_g(1)\otimes H_g(1)$ (see Table II). Both of these $(Ph_4P)_2IC_{60}$ modes are slightly redshifted from the known C_{60} frequencies (273 and 533 cm^{-1}),[42] and both appear as weak doublets at low T (the overtone mode is extremely weak at low T and not detected at RT). In support of these assignments, recent Raman data on $(Ph_4P)_2IC_{60}$ show that the $H_g(1)$ mode is split and redshifted to $\approx$260 cm^{-1}.[48] At the same time, the usual $H_g(2)$ mode at 431 cm^{-1} appears in neither the Raman[48] nor FIR data.

We are successful in assigning four out of the five activated C_{60}^- modes in Table II, but the origin of the 504 cm^{-1} mode is much more difficult to identify. The even-symmetry $A_g(1)$ and $F_{1g}(1)$ modes are the only good candidates from among the C_{60} vibrations (Table II), but there is no theoretical justification for either of these modes to appear in the IR spectrum. Furthermore, the actual frequencies of these modes may differ from those shown in Table II: $A_g(1)$ appears at $\approx$490 cm^{-1} in the Raman data[48] and the location of $F_{1g}(1)$ in C_{60} is disputed.[41,42] Whereas the softening trend of the 504 cm^{-1} feature is typical of the C_{60}^- modes, the unique temperature behaviors of the linewidth and intensity differentiate it from those modes. Finally, the relative strength of the 504 cm^{-1} mode makes its activation from an even-symmetry mode seem unlikely. Alternative origins of the 504 cm^{-1} vibration include a large frequency shift of an existing counterion mode or activation of a new counterion mode. A remote possibility is large splitting and redshift of $F_{1u}(1)$.

B. The Jahn-Teller effect and electron-phonon coupling

As a molecule of high symmetry and degenerate electronic levels, the fulleride monoanion is subject to a Jahn-Teller effect (JTE) which stabilizes the molecule in a lower energy vibronic state.[19,49] A JT state is inherently dynamic because it consists of a set of equivalent lower symmetry conformations, over which the molecule is delocalized. For example, the D_{5d} distortion of the anion ball has five equivalent orientations.[20] In the case of strong JT coupling, potential wells exist at each conformational orientation and the molecule tunnels between them with some characteristic tunneling frequency that increases with temperature.[49] In the solid state, random local strain or crystal-field perturbations may lock the molecule in a given orientation of the distortion, resulting in a ''static'' JTE.[50] FIR techniques cannot distinguish between a static distortion and a dynamic distortion in the limit of strong coupling,[51] so we postpone consideration of that distinction until a later comparative discussion of other experimental work.

By theoretical consensus, the JT stabilization energy of C_{60}^- is expected to be small, due to delocalization of the extra electron over a large molecule.[19–23,52] As a result, the distortion of the ball can be treated as a perturbation on the original icosahedral symmetry, and the correlations between vibrational modes of the icosahedral and reduced symmetry point groups can be worked out by standard group theory. Table III lists the odd vibrations of the D_{5d}, D_{3d}, and D_{2h} point groups, derived from the parent icosahedral modes. In parentheses are the splittings, which indicate the multiplicity of resulting IR-active modes, as determined by selection rules. Comparison of predicted and actual splitting patterns will allow us to discriminate between different lower symmetry states. This perturbative approach was also successfully applied to confirm the reduced symmetry point groups of polymeric RbC_{60} and rhombohedral C_{60}.[34]

From the doublet splitting observed in $F_{1u}(1)$ and $F_{1u}(2)$ (Table II) and the splittings predicted by group theory (Table III), we determine that the C_{60}^- anion symmetry in $(Ph_4P)_2IC_{60}$ is reduced to D_{5d} or D_{3d},[53] and *not* D_{2h}. The narrow FIR linewidths are consistent with a single distortion rather than a competition between the reduced symmetry point groups,[20] although the D_{5d} and D_{3d} splitting energies might be so close as to avoid significant line broadening. The experimentally observed weak splittings of the F_{1u} modes ($2-7$ cm^{-1}) support the assumption of a small distortion of the C_{60}^- ball.

TABLE III. Correlation table of I_h symmetry group and subgroups.

I_h	D_{5d}	D_{3d}	D_{2h}
$1A_u$	$1A_{1u}$	$1A_{1u}$	$1A_u$
	$(0\rightarrow 0)$	$(0\rightarrow 0)$	$(0\rightarrow 0)$
$4F_{1u}$	$4A_{2u}+4E_{1u}$	$4A_{2u}+4E_u$	$4B_{1u}+4B_{2u}+4B_{3u}$
	$(1\rightarrow 2)$	$(1\rightarrow 2)$	$(1\rightarrow 3)$
$5F_{2u}$	$5A_{2u}+5E_{2u}$	$5A_{2u}+5E_u$	$5B_{1u}+5B_{2u}+5B_{3u}$
	$(0\rightarrow 1)$	$(0\rightarrow 2)$	$(0\rightarrow 3)$
$6G_u$	$6E_{1u}+6E_{2u}$	$6A_{1u}+6A_{2u}+6E_u$	$6A_u+6B_{1u}6B_{2u}+6B_{3u}$
	$(0\rightarrow 1)$	$(0\rightarrow 2)$	$(0\rightarrow 3)$
$7H_u$	$7A_{1u}+7E_{1u}+7E_{2u}$	$7A_{1u}+14E_u$	$14A_u+7B_{1u}+7B_{2u}+7B_{3u}$
	$(0\rightarrow 1)$	$(0\rightarrow 2)$	$(0\rightarrow 3)$
IR total			
$4(F_{1u})$	$26(A_{2u},E_{1u})$	$44(A_{2u},E_u)$	$66(B_{1u},B_{2u},B_{3u})$

In addition to splitting the original IR-active modes, JT symmetry-lowering also serves to activate previously silent modes (see Table III). Such activation is expected to obey strict complementarity of IR- and Raman-active modes since both D_{5d} and D_{3d} point groups retain an inversion center. On this basis, we attribute only odd modes to the Jahn-Teller distortion (an activation mechanism of even modes is discussed below). In principle, the D_{5d} and D_{3d} point groups are distinguishable by the degree of splitting of the activated (previously silent) fundamentals, but the far-infrared results are inconsistent on this point. The weak $F_{2u}(1)$ singlet at 351 cm^{-1} implies D_{5d} symmetry while the stronger $G_u(1)$ doublet at 398 cm^{-1} implies D_{3d} symmetry (see Table III), as does the weak $H_u(3)$ doublet at 665 cm^{-1}. (Possibly, the 351 cm^{-1} mode is too weak for any splitting to be detectable.) While the activation of even modes in the IR spectrum cannot be attributed to the lower symmetry point group, the splitting of the $H_g(1)$ modes (Table II) is another indication of the reduced symmetry of the anion. Since triplet splitting of H_g modes is predicted by group-theoretical analysis for both D_{5d} and D_{3d} (weak doublets are observed), these modes do not aid in distinguishing between the reduced symmetry states.

Doublet splitting of the F_{1u} modes and activation of previously silent modes are strong evidence of a RT Jahn-Teller distortion of the anion ball in $(Ph_4P)_2IC_{60}$. In contrast, single-crystal diffraction studies indicate a symmetric ball at room temperature, although the bond length alternation is not resolved.[4,5] We believe the structural result is consistent with the small bond length adjustments expected in the distorted ball[20–23,52] and with substantial local disorder present in $(Ph_4P)_2IC_{60}$ (free rotations of the ball,[10] orientational disorder,[4,5] and likely multiple static or dynamic JT conformations of the ball[20,49]).

The question remains, however, as to the static or dynamic nature of the distortion. CW EPR results indicate a RT dynamic JTE (symmetric ball) based on an isotropic g factor at 300 K.[6,11] On the other hand, the FIR results clearly show a room-temperature distortion of the ball. This seeming inconsistency can be reconciled if we consider the characteristic measurement frequencies of these techniques.[19,49] The relevant FIR vibrational frequencies are of the order 10^{13} s^{-1}, whereas the resonance transition frequencies measured by EPR occur at $\leqslant 10^9$ s^{-1}.[49] Measurement frequencies which are greater than the JT tunneling frequency $(1/\tau)$ sample an individual distortion of the ball, while frequencies less than $1/\tau$ average over many distortions, thereby restoring the original high symmetry of the molecule. If the tunneling frequency satisfies $10^9 < 1/\tau < 10^{13}$ s^{-1}, then the FIR and EPR results are consistent. We therefore take the experimental frequency values as upper and lower and bounds on a magnitude of $1/\tau$. In this scenario, the ball undergoes many ordinary vibrations between tunneling events, while numerous tunneling events (reconformations of the ball) occur during the span of a single resonance transition. Note, however, that although the FIR data do not contradict the EPR finding of a dynamic JTE at room temperature, they are equally consistent with a static distortion.

Appearance of a JT distortion (static or dynamic) in the FIR spectrum implies strong coupling of the JT-active H_g modes to the t_{1u} electronic levels.[51] In the static case, strong coupling is required to lock in the distortion, and in the dynamic case the coupling must be strong enough ($1/\tau$ low enough) that vibrational modes of the distorted molecule acquire sufficient intensity to be observed. Early calculations yielded weak-coupling constants for most H_g modes of C_{60}^-,[54] but more recent experiments estimate moderate-to-strong coupling,[55] consistent with these FIR results. On the other hand, Jahn-Teller molecules are particularly susceptible to low-symmetry effects of the solid environment (e.g., strain or crystal-field perturbations) which can amplify the distortion.[49,50] Such extrinsic effects may play a significant role in $(Ph_4P)_2IC_{60}$, in the form of random strains introduced by the mixed occupancy of halide sites[14] or the less-than-cubic symmetry environment of the C_{60}^- anions.[4,5] Therefore, although our results are consistent with other recent work on C_{60}^-,[55] we cannot deduce intrinsic strong coupling in the C_{60}^- anion based on this study alone.

In addition to absorptions of the Jahn-Teller-distorted molecule, other evidence of electron-phonon coupling can appear in the IR spectrum. For example, coupling between H_g-derived phonons and inter-t_{1u}-band excitations in K_3C_{60} produces anomalous IR activity of broadened H_g modes (weakly allowed due to orientational disorder).[18,46,56] Although this coupling mechanism was derived for the metallic

TABLE IV. Temperature dependence of major FIR features.

$(Ph_4P)_2IC_{60}$ mode (cm^{-1})	Assignment	T dependence with decreasing T
90, 110, 135	Combination modes	All harden
398 (LT doublet)	$G_u(1)$	Splits below 150 K High ν side flat, low ν side softens
504 (singlet)	C_{60}^-? or counterion?	Flat, then softens below 125 K
525 (RT doublet)	$F_{1u}(1)$	High ν side hardens, flattens below 125 K Low ν side obscured
527 (LT doublet)	Counterion	High ν side hardens, inflection point near 150 K Low ν side independent of T
576 (RT doublet)	$F_{1u}(2)$	High ν side hardens, inflection point near 150 K Low ν side hardens then softens below 150 K

alkali fullerides,[46] we see its effect manifest in $(Ph_4P)_2IC_{60}$ (Ref. 57) in the weak activation of the $H_g(1)$ mode and its overtone, $H_g(1)\otimes H_g(1)$ (broadening of $H_g(1)$ is apparent in the Raman data[48]). In comparison, only the higher frequency H_g modes were observed in the IR spectrum of K_3C_{60},[56] but this difference probably can be attributed to different coupling in the singly and triply charged anions. The absence of $H_g(2)$ in both the Raman and IR data of $(Ph_4P)_2IC_{60}$ may be due to especially strong coupling of that mode,[55] causing its broadening and disappearance into the background.[56]

The F_{1u} modes, as well, are subject to electron-phonon coupling effects when the C_{60} ball acquires excess charge. In the A_nC_{60} compounds, $F_{1u}(4)$ undergoes a strong redshift and intensity increase while $F_{1u}(2)$ redshifts only slightly but exhibits a strong broadening.[18,58] This mode-selective dependence is explained mainly by different contributions of electron transfer and structural relaxation in the two modes, with solid-state effects (such as molecular deformations) having minor impact.[58] In $(Ph_4P)_2IC_{60}$, similar dramatic changes are observed in $F_{1u}(4)$,[8,12] whereas $F_{1u}(2)$ appears unaffected. We suspect that the lack of broadening or redshift of $F_{1u}(2)$ in $(Ph_4P)_2IC_{60}$ may be due to very different and increased solid-state effects in this particular fulleride salt, resulting from the presence of the large organic cations. The importance of such effects in $(Ph_4P)_2IC_{60}$ is reinforced by the absence of doublet splitting of F_{1u} modes[59] in fcc RbC_{60},[36,38] indicating that the JT distortion may not be observable unless amplified by the crystalline environment. Reduced intermolecular effects, common to both Rb_4C_{60} and $(Ph_4P)_2IC_{60}$, may also be a prerequisite for the JTE to be observed.[32]

C. Temperature dependence

Table IV summarizes the temperature dependences of the strongest features seen in the FIR spectrum of $(Ph_4P)_2IC_{60}$. Although the temperature dependences vary widely, some patterns emerge in the frequency behavior of the C_{60}^- intramolecular modes. These include a weak transition in the 125–150 K region and anomalous softening with decreasing temperature, which may correlate with the radial character of the modes.

The hardening of combination modes and some intramolecular modes is easily accounted for by lattice stiffening at low temperatures. Softening of other anion modes is less easily understood but follows a general pattern which might help explain it. The low ν sides of the doublets soften more than the high ν sides, and the lower frequency modes show more softening than higher frequency modes. These trends suggest an association of softening with degree of radial character of the mode, as proposed to explain the unique softening of $F_{1u}(1)$ in C_{60} films.[60] Indeed, normal mode calculations of C_{60} find 83, 93, and 67 % radial character of $G_u(1)$, $F_{1u}(1)$, and $F_{1u}(2)$, respectively.[61] These values are consistent with less overall softening observed in $F_{1u}(2)$ compared to the lower frequency (more radial) modes.[62] A normal coordinate analysis of the D_{5d} or D_{3d} distorted ball (in particular, the A_u and E_u or E_{1u} eigenvectors and energies) is not currently available, but might shed light on behavior differences of the high and low ν sides of the doublets in $(Ph_4P)_2IC_{60}$.

There is evidence of a weak transition between 125 and 150 K in the temperature dependences of the 398 cm^{-1} mode and the low ν side of the 576 cm^{-1} doublet, in particular. Splitting of the 398 cm^{-1} mode below 150 K (Fig. 4) suggests a symmetry reduction of the anion brought about by a phase transition. Such multiplet splitting is known to coincide with structural phase transitions, as in the orientational ordering transition of C_{60} at 260 K.[60,64] Further evidence of a weak transition appears in the change of slope of $\nu(T)$ near 150 K in the low ν side of the 576 cm^{-1} mode. The sensitivity of this $F_{1u}(2)$-derived vibration to some sort of transition is reminiscent of that mode's behavior in pristine C_{60}, where it exhibits uniquely sharp transitions in both frequency and linewidth at the rotational-ordering transition temperature.[60] The latter transition is much stronger (e.g., the frequency shifts abruptly) than the one we observe in $(Ph_4P)_2IC_{60}$, so it is not surprising that the dramatic narrowing behavior observed in the neutral material is not reproduced in the salt.[63]

The $\nu(T)$ behaviors of the other intramolecular C_{60}^- modes are less dramatic but still show anomalies in the 125–150 K region, supporting our claim of a weak phase transition there. These other modes include the high ν side of $F_{1u}(1)$ (Fig. 3) and the low ν side of $F_{1u}(2)$ (Fig. 2), as well as $F_{2u}(1)$, as described in Sec. III B. In addition, several counterion modes exhibit T dependences consistent with such a transition, in particular the 530 cm^{-1} mode (Fig. 3).

The involvement of counterion modes implies that the transition is not limited to the C_{60}^- ball, but is probably a bulk phenomenon.

A recently reported 140 K transition, observed in CW EPR studies of $(Ph_4P)_2IC_{60}$,[6,11] coincides neatly with the transition observed in this FIR work. While the former was attributed to a JT dynamic-to-static transition, we find we cannot naively adopt the same explanation of the FIR results, and must, in fact, re-evaluate the EPR transition as well. Typically, a dynamic-to-static transition is observed due to temperature dependence of the tunneling barrier height, causing a change in the relative magnitudes of the tunneling and measurement frequencies as T decreases.[49,50] Since the transition occurs at the temperature where the two magnitudes become equal, the transition temperature depends on the experimental measurement frequency. Because FIR and EPR frequencies are so vastly different, no such transition could be common to both experimental techniques. Moreover, no transition of this type could appear in the FIR results since the FIR frequencies already exceed $1/\tau$ at room temperature, allowing the individual distortion to be observed.

We briefly speculate on alternative explanations of the transition near 140 K which can account for its appearance in both EPR and FIR results, as well as for its absence in x-ray diffraction, specific heat, and differential scanning calorimetry studies.[5,7,11,65] One possible scenario is a dynamic RT competition between the D_{5d} and D_{3d} distortions[20] that resolves to D_{3d} alone below the transition temperature (presumably due to a small energy advantage in the D_{3d} distortion). This type of transition could produce the singlet-to-doublet splitting observed in the G_u-derived mode below 150 K (Fig. 4). Assuming the D_{3d} distortion provides greater stabilization of the ball, it will also have a lower tunneling frequency[51] and could therefore bring about the transition seen by EPR. X-ray-diffraction experiments would not perceive this type of molecular transition because local orientational disorder would obscure the symmetry changes of the ball, assuming persistence of static disorder at low T. It is not clear, however, that such a transition could induce the anomalous temperature dependences of the other C_{60}^- modes, nor would it affect the dynamics of the counterions.

To better account for the bulk aspect of the transition, the above molecular transition must be accompanied or driven by some sort of structural transition which induces interactions between anions and counterions. We suggest freezing out of the dynamic orientational disorder as one possibility. Recall that the local disorder consists of two equivalent 90 degree orientations of the ball. Below an orientational ordering transition, the newly static nature (and enhanced strength) of interactions between ball and slightly anisotropic counterion environment might be sufficient to favor the D_{3d} distortion over the D_{5d}, and to lock in a single distortion at each orientation. The two lines (anisotropic g factor) seen in EPR measurements below 140 K would thus be accounted for.[6,11] Presumably, anion-counterion interactions also could have small affects on the vibrational frequencies of other modes, thus explaining the FIR T-dependent results. Although no orientational ordering transition appears in the x-ray diffraction studies,[65] recent diffuse x-ray scattering data on $(Ph_4P)_2BrC_{60}$ show changes in the orientational disorder near 100 K.[66]

V. CONCLUSION

In conclusion, we have made high-resolution FIR transmission measurements on the radical anion salt, $(Ph_4P)_2IC_{60}$, to study the dynamics of the singly charged anion ball. We find a D_{5d} or D_{3d} distortion of the C_{60}^- ball at room temperature, manifest in doublet splitting of the $F_{1u}(1)$ and $F_{1u}(2)$ modes and activation of silent odd modes. This result is consistent with a dynamic Jahn-Teller distortion (in the case of strong coupling), as suggested by recent EPR studies, or with a static distortion stabilized by low-symmetry perturbations. The activation of H_g modes is attributed to electron-phonon coupling in the presence of orientational disorder.

We follow the detailed temperature dependences of the strongest FIR features. They reveal a weak transition in the region 125–150 K which cannot be accounted for by temperature dependence of the JT tunneling frequency. Evidence of the transition in counterion modes points to a bulk, rather than molecular, effect, produced by C_{60}^--counterion interactions. Several C_{60}^- modes exhibit anomalous softening with decreasing temperature, which may correlate with the degree of radial character of these vibrations.

ACKNOWLEDGMENTS

We are grateful to the Division of International Programs of the National Science Foundation (Grant No. INT-9722488), the Division of Materials Research of the National Science Foundation (Grant No. 9623221), the Hungarian National Science Foundation (Grant No. OTKA T22404), and the National Research Council's Collaboration in Basic Science and Engineering Program for their generous support of this research. We thank Danilo Romero for the C_{60} film sample and Jerzy Janik, Daniel Kahn, and Peter Zavalij for helpful discussions about this work.

[1] H. W. Kroto, J. R. Heath, S. C. O'Brien, R. F. Curl, and R. F. Smalley, Nature (London) **318**, 162 (1985).

[2] W. Krätschmer, L. D. Lamb, K. Fostiropoulos, and D. R. Huffman, Nature (London) **347**, 354 (1990).

[3] M. S. Dresselhaus, G. Dresselhaus, and P. C. Eklund, *Science of Fullerenes and Carbon Nanotubes* (Academic, New York, 1996).

[4] A. Pénicaud, A. Peréz-Benítez, R. Gleason V., E. Muñoz P., and R. Escudero, J. Am. Chem. Soc. **115**, 10 392 (1993).

[5] U. Bilow and M. Jansen, J. Chem. Soc. Chem. Commun. **1994**, 403.

[6] B. Gotschy, M. Keil, H. Klos, and I. Rystau, Solid State Commun. **92**, 935 (1994).

[7] H. Klos, W. Brütting, A. Schilder, W. Schütz, B. Gotschy, G. Völkel, B. Pilawa, and A. Hirsch, in *Progress in Fullerene Research*, edited by H. Kuzmany, J. Fink, M. Mehring, and S. Roth

(World Scientific, Singapore, 1994), p. 297.
[8] K. Kamarás, D. B. Tanner, L. Forró, M. C. Martin, L. Mihaly, H. Klos, and B. Gotschy, J. Supercond. **8**, 621 (1995).
[9] V. N. Semkin, N. G. Spitsina, S. Król, and A. Graja, Chem. Phys. Lett. **256**, 616 (1996).
[10] W. Scheinast, A. Schilder, W. Schütz, and B. Gotschy, in *Fullerenes and Fullerene Nanostructures*, edited by H. Kuzmany, J. Fink, M. Mehring, and S. Roth (World Scientific, Singapore, 1996), p. 544.
[11] B. Gotschy and G. Völkel, Appl. Magn. Reson. **11**, 229 (1996).
[12] A. Graja, V. N. Semkin, N. G. Spitsina, and S. Król, in *Electrical and Related Properties of Organic Solids*, edited by R. W. Munn, A. Miniewicz, and B. Kuchta (Kluwer, Dordrecht, 1997), p. 259.
[13] Unpublished results cited in (Ref. 12) claim a triclinic space group with very similar *a* and *b* lattice constants.
[14] W. Schütz, J. Gmeiner, A. Schilder, G. Gotschy, and V. Enkelmann, J. Chem. Soc. Chem. Commun. **1996**, 1571.
[15] W. Schütz, Ph.D. thesis, University of Bayreuth, 1996.
[16] K. Kamarás, M. Matsumoto, M. Wojnowski, E. Schönherr, H. Klos, and B. Gotschy, in *Progress in Fullerene Research* (Ref. 7), p. 357.
[17] M. J. Rice and H.-Y. Choi, Phys. Rev. B **45**, 10 173 (1992).
[18] T. Pichler, R. Winkler, and H. Kuzmany, Phys. Rev. B **49**, 15 879 (1994).
[19] C. C. Chancey and M. C. M. O'Brien, *The Jahn-Teller Effect in C_{60} and Other Icosahedral Complexes* (Princeton University Press, Princeton, 1997).
[20] N. Koga and K. Morokuma, Chem. Phys. Lett. **196**, 191 (1992).
[21] K. Tanaka, M. Okada, K. Okahara, and T. Yamabe, Chem. Phys. Lett. **193**, 101 (1992).
[22] W. F. Green, Jr., S. M. Gorun, G. Fitzgerald, P. W. Fowler, A. Ceulemans, and B. C. Titeca, J. Phys. Chem. **100**, 14 892 (1996).
[23] V. de Coulon, J. L. Martins, and F. Reuse, Phys. Rev. B **45**, 13 671 (1992).
[24] A. J. Schell-Sorokin, F. Mehran, G. R. Eaton, S. S. Eaton, A. Viehbeck, T. R. O'Toole, and C. A. Brown, Chem. Phys. Lett. **195**, 225 (1992).
[25] T. Kato, T. Kodama, and T. Shida, Chem. Phys. Lett. **205**, 405 (1993).
[26] J. Stinchcombe, A. Pénicaud, P. Bhyrappa, P. D. W. Boyd, and C. A. Reed, J. Am. Chem. Soc. **115**, 5212 (1993).
[27] J. Fulara, M. Jakobi, and J. P. Maier, Chem. Phys. Lett. **116**, 3465 (1994).
[28] M. M. Khaled, R. T. Carlin, P. C. Trulove, G. R. Eaton, and S. S. Eaton, J. Am. Chem. Soc. **211**, 227 (1993).
[29] H. Kondo and K. Morokuma, Chem. Phys. Lett. **237**, 111 (1995).
[30] Far-infrared measurements exhibited no magnetic field dependence. A. Ziebold and D. B. Tanner (unpublished results).
[31] G. Völkel, A. Pöppl, J. Simon, J. Hoentsch, S. Orlinskii, H. Klos, and B. Gotschy, Phys. Rev. B **52**, 10 188 (1995).
[32] R. Kerkoud, P. Auban-Senzier, D. Jérome, S. Brazovskii, I. Luk'yanchuk, N. Kirova, F. Rachdi, and C. Goze, J. Phys. Chem. Solids **57**, 143 (1996).
[33] P. W. Stephens, L. Mihaly, J. B. Wiley, S.-M. Huang, R. B. Kaner, F. Dietrich, R. L. Whetten, and K. Holczar, Phys. Rev. B **45**, 543 (1992).
[34] K. Kamarás, Y. Iwasa, and L. Forró, Phys. Rev. B **55**, 10 999 (1997).
[35] K. Kamarás, S. Pekker, D. H. Tanner, and L. Forró, in *Fullerenes and Fullerene Nanostructures* (Ref. 10), p. 119.
[36] M. C. Martin, D. Koller, A. Rosenberg, C. Kendziora, and L. Mihaly, Phys. Rev. B **51**, 3210 (1995).
[37] M. Núñez-Regueiro, L. Marques, J.-L. Hodeau, O. Béthoux, and M. Perroux, Phys. Rev. Lett. **74**, 278 (1995).
[38] H. Kuzmany, R. Winkler, and T. Pichler, J. Phys.: Condens. Matter **7**, 6601 (1995).
[39] Paraffin is clear in the far infrared except for a narrow feature at 79 cm^{-1}.
[40] The period of the fringes is consistent with the 10^{-1} mm thickness of the pellet, indicating that the fringes result from the smooth parallel plate surfaces of the pellet.
[41] K.-A. Wang, A. M. Rao, P. C. Eklund, M. S. Dresselhaus, and G. Dresselhaus, Phys. Rev. B **48**, 11 375 (1993).
[42] M. C. Martin, X. Du, J. Kwon, and L. Mihaly, Phys. Rev. B **50**, 173 (1994).
[43] M. C. Martin, J. Fabian, J. Godard, P. Bernier, J. M. Lambert, and L. Mihaly, Phys. Rev. B **51**, 2844 (1995).
[44] Ph_4PI is hygroscopic, and although care was taken to limit exposure to air and reduce effects of moisture, it is possible that these low-energy modes are related to water adsorption.
[45] Asymmetry in the peak shapes precluded making fits of sufficient accuracy to reproduce the very small changes in frequency with temperature.
[46] M. J. Rice, H.-Y. Choi, E. J. Mele, and M. Deshpande, Phys. Rev. B **49**, 3687 (1994).
[47] Symmetry-breaking crystal-field effects may also weakly activate even-symmetry modes in the IR spectrum (Ref. 43), but we saw no indication of this in $(Ph_4P)_2IC_{60}$.
[48] J. L. Sauvajol, A. Graja, L. Firlej, and S. Król, J. Mol. Struct. **436**, 19 (1997).
[49] I. B. Bersuker, *The Jahn-Teller Effect and Vibronic Interactions in Modern Chemistry* (Plenum, New York, 1984).
[50] A. Abragam and B. Bleaney, *Electron Paramagnetic Resonance of Transition Ions* (Clarendon, Oxford, 1970).
[51] W. R. Thorson, J. Chem. Phys. **29**, 938 (1958).
[52] F. Negri, G. Orlandi, and F. Zerbetto, Chem. Phys. Lett. **144**, 31 (1988).
[53] Likely low T $F_{1u}(3)$ and $F_{1u}(4)$ doublets, in the unpublished data of Kamarás *et al.*, support our deduction of a D_{5d} or D_{3d} point group. In addition, the asymmetrical peak shape of $F_{1u}(4)$ required a doublet for satisfactory fitting of that mode in the RT data of Semkin *et al.* (Ref. 9).
[54] C. M. Varma, J. Zaanen, and K. Raghavachari, Science **254**, 989 (1991).
[55] O. Gunnarsson, H. Handschuh, P. S. Bechthold, B. Kessler, G. Ganteför, and W. Eberhardt, Phys. Rev. Lett. **74**, 1875 (1995).
[56] T. Pichler, R. Matus, and H. Kuzmany, Solid State Commun. **86**, 221 (1993).
[57] $(Ph_4P)_2IC_{60}$ is a semiconductor, but we believe the model of Rice *et al.* (Ref. 46) is still applicable because the interband coupling of the H_g phonons is separated by symmetry from the intraband (Drude) part of the electronic polarizability.
[58] P. Giannozzi and W. Andreoni, Phys. Rev. Lett. **76**, 4915 (1996).
[59] It is possible that the required high measurement temperatures in fcc RbC_{60} may obscure the weak doublet splittings we observe in $(Ph_4P)_2IC_{60}$.
[60] J. Onoe and K. Takeuchi, J. Phys. Chem. **99**, 16 786 (1995).
[61] R. E. Stanton and M. D. Newton, J. Phys. Chem. **92**, 2141 (1988).
[62] The tangential mode, $F_{1u}(4)$, also softens significantly with de-

creasing T in the unpublished data of Kamarás *et al.*, which is counter to the trend described for the low-frequency modes. Such inconsistencies in the behaviors of high- and low-frequency modes also appear in pressure dependence studies (Ref. 3).

[63] No indication of a transition appears in the temperature dependences of the F_{1u} peak intensities in either $(Ph_4P)_2IC_{60}$ or pristine C_{60} (Ref. 60).

[64] K. Kamarás, L. Akselrod, S. Roth, W. Hönle, and H. G. von Schnering, Chem. Phys. Lett. **214**, 338 (1993).

[65] U. Bilow and M. Jansen, Z. Anorg. Allg. Chem. **621**, 982 (1995).

[66] P. Launois and R. Moret (personal communication).